BACK-CALCULATIONS OF OBSERVED AVALANCHES AGAINST NATURAL DEFLECTING DAMS

Dieter Issler[1] Carl B. Harbitz[1] Ulrik Domaas[1] Kalle Kronholm[1] Marc Christen[2]
[1]Norwegian Geotechnical Institute, P.O. Box 3930 Ullevål Stadion, 0806 Oslo, Norway
[2]WSL Institute for Snow and Avalanche Research SLF, 7260 Davos Dorf, Switzerland

ABSTRACT: The objective of this study is to assess the reliability of presently available numerical avalanche models in predicting avalanche flow about deflecting natural terrain features such as large boulders or moraine ridges. Field observations from Norway have been back-calculated using RAMMS. The observations vary in quality, but the main features of the avalanches regarding release, track and runout have been documented. The quality of the available digital elevation model is critical for the model results. For the two smallest avalanches, good agreement between simulation and observation of both run-up height and runout distance required substantially higher values than commonly used for the friction parameters μ and ξ. This has the effect of increasing the velocity in the track and shortening the stopping distance.

1 INTRODUCTION

Dynamical models of snow avalanche motion have become an indispensable tool in avalanche hazard mapping and the design of countermeasures. In recent years, a number of quasi-three-dimensional models (Q3DMs) have begun to replace the Q2DMs that had been in use since the 1980s. Q3DMs have the obvious advantage that they *calculate* the path the avalanche takes while the user has to choose it before the calculation in Q2DMs. Moreover, Q3DMs take into account the variable width of an avalanche, which is also an important factor in channeled tracks, in runout on alluvial fans, and in determining the run-up height (and possible spilling-over) in bends.

The present numerical models need extensive calibration because they are not able to calculate avalanche motion from first principles, using only directly measurable snow properties as input. Important processes like snow entrainment, inter-particle collisions and comminution and/or coalescence of particles are incompletely described or neglected. Hence, the model parameters do not directly correspond to physical processes—e.g. the dry-friction parameter μ appearing in most models is much smaller than the friction coefficient of snow on snow (Casassa et al., 1989). Most of the data that is available for model calibration consists of observed runout distances. Velocity was measured only at a few test sites, and the initial conditions—release area, fracture depth and snow properties—have rarely been determined. It has been known for a long time (Gubler, 1987) that traditional calibrations based on runout distance (Buser and Frutiger, 1980; Martinelli, Jr. et al., 1980; Gruber, 1998) often lead to severe underestimation of the velocity over large parts of the track, with obvious consequences for the design of avalanche protection dams.

With this state of affairs, it is interesting to test presently available Q3DMs against well-documented avalanche events where the topography caused large deflection of the flow and the run-up height could be determined. Two of the authors surveyed fifteen sites in Norway where such events had happened (Harbitz and Domaas, 2011). Among them, we selected three that we expected to be particularly discriminating and for which the initial conditions can be reconstructed with different degrees of confidence (Sect. 3). Admittedly, significant uncertainty remains in all three cases: Most of the surveys took place long after the event so that the release area could rarely be measured directly. Also, reports by lay persons do not differentiate between different flow regimes. Furthermore, detailed meteorological measurements at high altitude are almost inexistent in Norway.

For a numerical model, we chose RAMMS v.1.4.14 as a typical representative of Q3DMs, see Sect. 2 for a brief summary and (Christen et al., 2010) for

[0]*Corresponding author:* Dieter Issler, Norwegian Geotechnical Institute, P.O. Box 3930 Ullevål Stadion, 0806 Oslo, Norway; tel. +47-4698-7346; fax: +47-2223-0448; e-mail: di@ngi.no

more details. For a terrain model, the 15 m DEM covering all of Norway was interpolated to a grid spacing of 5 m. In the first round, we used standard friction parameters as recommended in Christen et al. (2011) for the corresponding avalanche category with respect to size, altitude, track type and (estimated) return period. Based on the results, we optimized—separately for each avalanche—the parameters so as to get the best match with the observations (Sect. 4). We discuss our findings in Sect. 5.

2 SUMMARY OF THE NUMERICAL MODEL

Q3DMs are based on the principle of conservation of mass and momentum. The flow variables (in this case the slope-parallel components of velocity, u and v) are integrated over the flow depth, h, which thereby itself becomes one of the dynamical variables:

$$\partial_t h + \partial_x(hu) + \partial_y(hv) = w_e, \tag{1}$$

$$\partial_t(hu) + \partial_x(f_m h u^2) + \partial_y(f_m v u) = h g_x + \partial_x\left(k_{a/p} f_p \frac{h^2}{2} g_z\right) - \hat{\tau}_b \frac{u}{U}, \tag{2}$$

$$\partial_t(hv) + \partial_x(f_m h u v) + \partial_y(f_m v^2) = h g_y + \partial_y\left(k_{a/p} f_p \frac{h^2}{2} g_z\right) - \hat{\tau}_b \frac{v}{U}. \tag{3}$$

(g_x, g_y, g_z) is the gravitational acceleration in a local coordinate system with z perpendicular to the slope. $\hat{\tau}_b$ denotes the magnitude of the specific bed shear stress in the flow direction, and $U \equiv (u^2 + v^2)^{1/2}$ is the speed. The shape coefficients f_m and f_p are set to 1 in RAMMS as the density and velocity profiles are assumed uniform (and constant) throughout the flow. $k_{a/p}$ is the earth-pressure coefficient, which generally takes on different values in active (extensional) and passive (compressional) states in RAMMS, but is set to 1 in this study.

Like many other models, RAMMS implements the Voellmy friction law (Voellmy, 1955), which combines particle-like (Coulomb friction, friction coefficient μ) and fluid-like behavior ("turbulent" drag, coefficient ξ):

$$\hat{\tau}_b = \mu h g_z + \frac{g}{\xi} U^2 \tag{4}$$

The values of μ and ξ have to be found through extensive calibration and are known to vary much along the path and between different avalanches because of (i) non-uniform terrain roughness (including forest stands), (ii) spatially varying snow properties such as particle size and water content, and (iii) other effects that are not properly represented in the model. RAMMS computes default values locally from avalanche size and return period, altitude and terrain curvature. They are typically in the range $\mu = 0.15$–0.40 and $\xi = 1000$–$2500\,\mathrm{m\,s^{-2}}$. We note that the Voellmy friction law gives an asymptotic speed of

$$U_{\max} = (\xi h(\sin\theta - \mu\cos\theta))^{1/2} \tag{5}$$

on a long slope with slope angle θ if the flow depth is assumed constant. Typically, $U_{\max}$ is of the order of 30 m/s.

The entrainment rate, w_e, on the right-hand side of Eq. (1) is set to 0 in the presently shipped version of RAMMS. Tests with a development version implementing a variant of the Grigorian–Ostroumov entrainment model indicated that inclusion of entrainment gives better agreement between measured and simulated velocities as well as reduced spread in the friction parameters (Sovilla et al., 2006). Nevertheless, we used the standard model without entrainment in this study.

These equations are solved numerically by discretizing them spatially over a grid of rectangular cells derived from a DEM (digital elevation model, with resolution typically 1–10 m) and in time (with timesteps typically in the range 0.001–0.1 s). The user has to specify the initial conditions (extent of the release zone, fracture depth, the spatial distribution of the friction parameters and—if entrainment is included—the depth of entrainable snow along the path.

Shear stresses on vertical planes cannot be determined without further assumptions and are neglected by RAMMS and most similar models, and so are curvature effects. While they are of little importance in avalanches over relatively smooth terrain, they are expected to influence avalanche behavior more strongly in sharp bends imposed by natural or man-made dams.

3 TEST CASES: AVALANCHES AGAINST NATURAL DAMS

The three avalanche events briefly described below are more fully documented in (Harbitz and Domaas, 1997, 2011). Table 1 summarizes some of the key

Figure 1: Vassdalen avalanche: Release area, track and deflecting slope seen from north-west. Oval indicates a flow-splitting ridge.

Figure 2: Gaukheidalen avalanche: Part of the release area and upper track with the deflecting shoulder. The approximate flow line of the avalanche is indicated with a line.

characteristics of the paths and lists our assessments of the most probable initial conditions of the simulated events.

Vassdalen 1986, Ankenes municipality. The event of 1986-03-05 was released remotely during army exercises and killed 16 soldiers. The circumstances of the catastrophe and the path properties are described by Lied (1988). Despite moderate dimensions (fall height 260 m), the avalanche fluidized to a significant degree. After descending on an open slope, the avalanche hit the bottom of a side valley at an angle of about 40°, ran up 25 m on the opposite slope (measured vertically from the side valley bottom) and maintained that height for 200 m (Fig. 1). The return period of this specific event is difficult to assess, but probably larger than 30 years.

Gaukheidalen, Brønnøy municipality. A small to medium-size avalanche was released in the winter of 1996 near the farm Bordvik in the municipality of Brønnøy, Nordland county; the survey took place in the subsequent summer. The open-slope release area with inclination from 30° to over 50° is oriented such that it collects considerable amounts of snow during snow showers under north-westerly winds. The avalanche completely destroyed a mixed forest stand from 200 m a.s.l. right to a 5 m high cliff where it was abruptly stopped. Between 190 and 125 m a.s.l., a curved shoulder deflects the avalanche at the same time as the track narrows rapidly. The run-up height on this shoulder could be measured fairly exactly (Fig. 2). When comparing with simulation results, one has to keep in mind that the extent of the deposits outside the damage area is not known. There is also considerable uncertainty about the initial conditions (extent of starting zone, fracture depth).

Indre Standal, Ørsta municipality. The municipality of Ørsta in the county of Møre og Romsdal (western Norway) comprises a great number of large avalanche paths. Due to the relatively high altitudes of many starting zones, high amounts of precipitation, a distance of 30–50 km from the coast and steep slopes, dry-snow avalanches with a significant suspension layer (“powder-snow avalanches”) are frequent.

Figure 3: Indre Standal, Ørsta municipality. The upper deflecting dam (“Standal Fortress”) is partly visible at the left edge of the picture. The outer curve of the lower deflecting dam appears as a bright area in the middle upper part of the picture (from SW).

Table 1: Main characteristics of avalanche paths used in this study and assumed initial conditions of simulated events. Observations are from (Harbitz and Domaas, 1997, 2011). Runout angle is measured from crown to toe of deposit. Expected runout angle is from α-β model (Lied and Bakkehøi, 1980). The two values given for Indre Standal avalanche refer to the upper and lower dam, respectively.

		Vassdalen	Gaukheidalen	Indre Standal
Climate zone		Transitional	Maritime	Transitional
Altitude a.s.l.	(m)	210–470	55–370	0–1200
Release zone slope	(°)	35	38.5	52
Release area	(m^2)	∼10,000	15,000(?)	60,000
Release zone		Slightly concave	Open slope	Bowl-shaped
Track		Valley flank, open slope, joining valley obliquely, then somewhat channeled.	Open to slightly channeled, S-curve, at end impact against small cliff.	Open slope to 125 m a.s.l., cliff 800–900 m a.s.l., below 100 m a.s.l. two gullies to fjord.
Terrain roughness	(m)	1–2	1–5	0.5–2
Avg. track angle β	(°)	25.8	26.9	38.4
Expected runout angle	(°)	23.4	24.4	35.5
Observed runout angle	(°)	20.5	25.5	36.0
Dam characteristics		Opposite valley flank, undulating.	Curved shoulder, curvature radius ∼150 m	Upper: splitter / deflector, funnel-shaped. Lower: curvature radius ∼150 m.
Impact angle horizontal	(°)	40	50	45 / 60
Dam inclination	(°)	45	35	45 / 20
Dam height	(m)	15–30	16	20 / 10
Observed run-up height	(m)	25	9	13 / 9
Estimated return period	(years)	>30	10–30	>20
Snowfall, 3 days	(m)	0.8	1.1	2.0
Snowdrift release zone	(m)	0.5	0.3	0.0
Estimated fracture depth	(m)	1.0	0.7	0.6
Estimated release volume	(m^3)	10,000	10,500	36,000

The steep path from the mountain Storhornet was surveyed in July 1997 after an event with an estimated return period of 10–30 years (smaller avalanches are released annually). The majority of avalanches probably originate between 1000 and 1200 m a.s.l. The total travel distance is 2200-2300 m down to the sea level. At about 125 m a.s.l., the avalanche is divided by a terrain formation, called the “Standal Fortress”, that acts both as a splitter and a deflecting dam, see Fig. 3. The main part of the avalanche is deflected east towards (and partly into) the fjord, while the minor western part of the avalanche continues straight on in a gully. Extensive damage to the surrounding forest is observed. The suspension layer sometimes causes damage to the houses on Indre Standal farm, 700 m past the top of the dam. The eastward deflected avalanche continues to a lower curve where the 1997 avalanche climbed over the natural deflecting dam and continued 85 m from the top of the dam in the direction the avalanche had prior to dam impact.

4 NUMERICAL SIMULATIONS

All simulations were carried out using the DEM that is available for all of Norway and is based on maps with 20 m equidistance. At 15×15 m^2 mesh size, the spatial resolution is nominally better than the minimum resolution suggested by Bühler et al. (2011). It is, however, insufficient to render small terrain features that can strongly influence avalanche behavior in the runout zone, like the 5 m high cliff that stopped the Gaukheidalen avalanche. Moreover, comparison of maps, DEM and orthophotos revealed significant discrepancies in all three test cases, particularly at and near the terrain features we are interested in.

Determining the initial conditions was a challenge for the Gaukheidalen and Indre Standal avalanches because direct observations from the release areas or estimates of the deposit volume are missing and the dates of the events are unknown. Based on the observed damage patterns and the state of the surrounding vegetation, the return periods were estimated. A comprehensive study of extreme precipitation values in Norway (Førland, 1992) provides a map of maximum 24-hours precipitation with return period five years, M5(24h), graphs for extrapolating to different intervals (72 hours in our application) and return periods, and indicates the approximate ratio between winter maximum precipitation and annual maximum precipitation (which is between 0.8 and 0.9 for all three sites). Taking into account altitude, slope angle, and wind exposure of the starting zones, approximate release depths can be estimated in a similar way as proposed in the Swiss guidelines (Salm et al., 1990). The resulting values are indicated in the bottom part of Table 1. Obviously, the uncertainty is large and propagates to the friction parameters μ and ξ. We modified the default altitude categories in RAMMS to account for the fact that isotherms and timberline are generally 1000–1500 m lower in Norway than in the Alps.

Vassdalen avalanche of 1986-03-05: The available digital maps and elevation model of the area proved to be much less accurate than the non-digital map that was used in the investigations after the accident (Lied, 1988). A little ridge below the starting zone, marked in Fig. 1, splits the flow to some degree, but the simulated eastern branch (right-hand side in flow direction) is deflected so much to the right that it overflows a much larger area of the opposite slope than registered on the map from 1986. It also causes numerical instabilities in the tail of the flow, connected to very small flow depths and causing unphysical "jets". Similar effects were observed in the simulations with a Q2DM by Irgens et al. (1998).

With RAMMS' built-in friction parameters, one has to assume a medium-size avalanche with a return period of 300 years in order to reproduce the observed run-up height reasonably well ($\mu = 0.18$–0.28, $\xi = 1400$–3000 m/s^2). But even so, the simulated runout distance on the plain remains too short (Fig. 4, left panel). The head of the avalanche is seen to spread too much sidewise. The maximum velocity of about 28 m/s is reached in the left branch between 320 and 270 m a.s.l.

Better agreement of the simulated and observed runout distance can be obtained by choosing $\xi = 30{,}000$ m/s^2 and $\mu = 0.32$ (Fig. 4, right panel), i.e., the Coulomb friction completely dominates. A Coulomb model with the effective friction coefficient μ chosen in agreement with the runout angle predicted by the α-β model (Lied and Bakkehøi, 1980) was advocated by Gauer et al. (2010) to better reconcile runout and velocity data. Here, this choice leads to a maximum velocity of about 38 m/s in the lower track. However, the right branch of the avalanche runs up far beyond the observed reach. Contrary to observations, the toe of the simulated avalanche is not deflected to the west—most likely due to the poor quality of the terrain model.

Gaukheidalen avalanche, 1996: At and near the deflecting dam, the map and the DEM appear to be at odds. This makes it difficult to compare the predicted and observed run-up heights objectively. However, the simulation with standard parameters, taking into account the braking effect of the forest ($\mu = 0.25$–0.34, $\xi = 300$–2000 m/s^2), falls short of the observed run-up heights (Fig. 5, left panel), while the lateral spreading in the deposit area probably is excessive. The early stopping of the left side of the avalanche, on the other hand, is partly reproduced. Using parameters corresponding to a very rare, large avalanche (not shown) has only a moderate effect on the run-up height because the extra "turbulent" drag in the forest keeps the velocity low.

As for the Vassdalen avalanche, runs with reduced drag and increased Coulomb friction (Fig. 5, right panel) lead to better agreement with observations. With $\mu = 0.40$, $\xi = 30{,}000$ m/s^2 above the forest and $\mu = 0.50$, $\xi = 10{,}000$ m/s^2 in the forest, the run-up height is only slightly overestimated, the avalanche

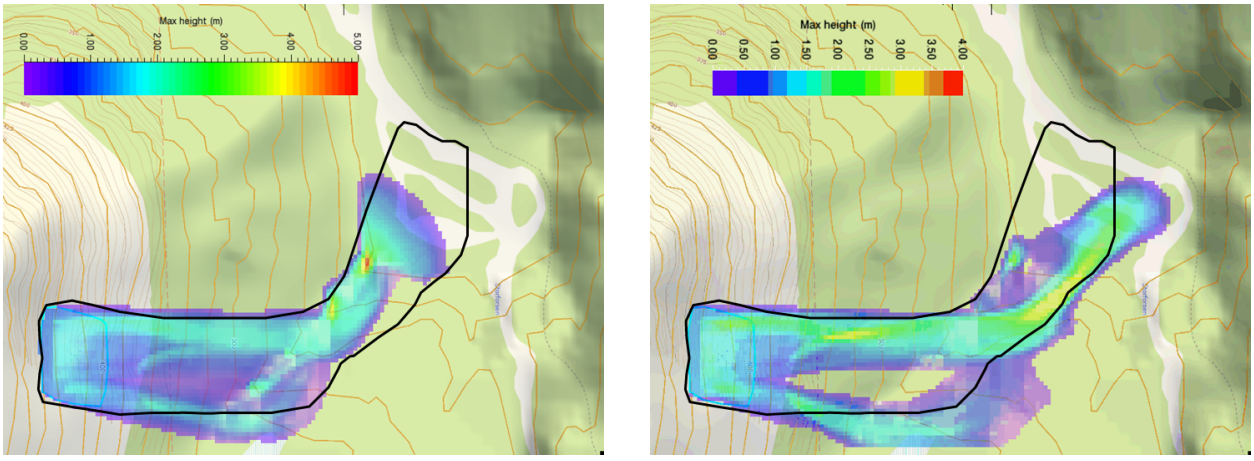

Figure 4: Vassdalen avalanche of 1986-03-05: Map showing observed outline of avalanche (black line) and distribution of maximum flow heights according to simulations with standard (left panel) and optimized parameters (right panel). North is to the right, scale 1:10,000, equidistance 20 m.

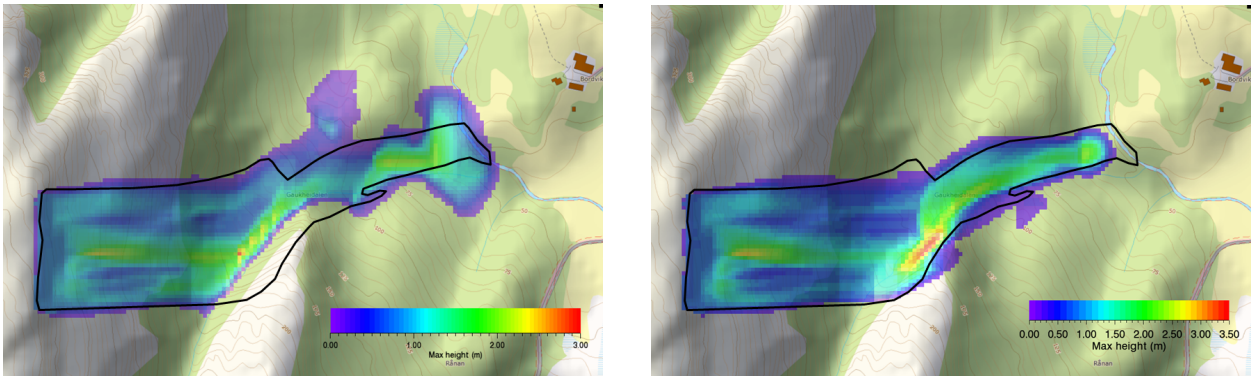

Figure 5: Gaukheidalen avalanche: Map showing observed extent of avalanche (black line) and simulated distribution of maximum flow height using standard (left panel) and optimized parameters (right panel). North is up, scale 1:10,000, equidistance 5 m.

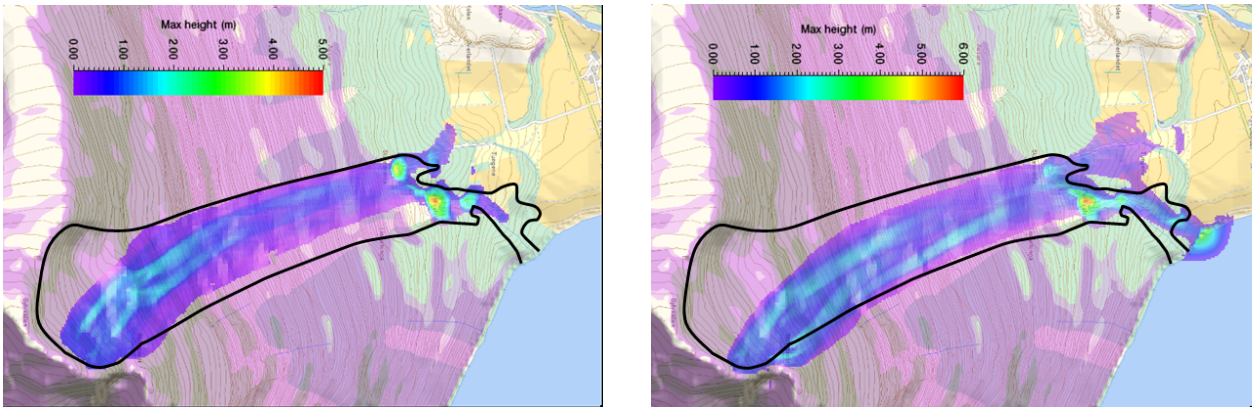

Figure 6: Simulations of 1997 Indre Standal avalanche with use of standard parameters (left panel, scale 1:35,000) and with increased release depth and reduced friction (right panel, scale 1:12,000). The black line indicates the outline of the observed event. North is to the right, scale 1:35,000, equidistance 5 m.

stops with less lateral spreading, and all the way the pressure is high enough to destroy the forest. The high value of ξ allows the avalanche to attain higher speed in the steep part of the track and to stop more abruptly at the end. High basal friction also suppresses the unphysical creeping motion due to the earth pressure gradient that persists in the simulations with standard parameters long after the avalanche essentially has come to a stop.

Indre Standal, 1997: The correspondence between DEM and topographic map is better than in the Vassdalen case, yet there may be a systematic discrepancy that causes the simulated avalanches to tend more to the left (west) than the avalanche flow traces visible on the orthophoto indicate. With standard friction parameters ($\mu = 0.22$–0.34, $\xi = 1300$–$2600\,\mathrm{m/s^2}$), the avalanche stops well before reaching the fjord (Fig. 6, left panel). When using Coulomb-model parameters $\mu = 0.65$, $\xi = 30{,}000\,\mathrm{m/s^2}$, the avalanche becomes too fast and overflows the "fortress" in a straight line (not shown). Choosing the release area far to the east under Storehornet's summit (where a release is expected to be much less likely), the simulated avalanches hit the "fortress" as observed in 1997. Best agreement with observations was found by increasing the release depth from 0.6 to 0.8 m and decreasing friction to the values corresponding to large avalanches with a return period of 300 years ($\mu = 0.15$–0.28, $\xi = 1500$–$3000\,\mathrm{m/s^2}$). With this, RAMMS reproduces the observed avalanche outline reasonably well (Fig. 6, right panel). The remaining discrepancies are most likely caused by (i) lack of detail in the terrain model, (ii) absence of visible damage at the outer fringes of the deposits, and/or (iii) a slight error (1–2 m/s) in the simulated velocity. A low value of μ seems to be key for reproducing runout of the right (eastern) branch to the fjord.

5 DISCUSSION AND CONCLUSIONS

The present study was conducted under circumstances that resemble the conditions in practical applications during consulting work: Little is known about the avalanche history of the studied paths, and it was not possible to conduct an exhaustive study because there are too many independent parameters that can be varied: The release area and the fracture depth are only approximately known, and RAMMS allows for independent values of μ and ξ for each cell of the mesh. Systematic scanning of the parameter space might yield parameter distributions that remedy the discrepancies we found. However, in all likelihood these would be strongly problem-dependent parameter sets that cannot readily be applied in other cases.

A major problem encountered in all three case studies is the quality of the DEM. When it comes to the small-scale behavior of avalanches—as is often the case in the design of mitigation measures—the resolution of the underlying DEM has to be commensurate with the required detail. The DEM quality ranged from good (Gaukheidalen) to insufficient (Vassdalen), despite the common source of the map data. This is probably not specific to Norway, and the situation will eventually improve.

The left panels of Figs. 4–6 indicate that calculations with the standard parameter choice built into RAMMS might have underestimated the runout distance in two of three cases, but it is uncertain whether this is due to a shortcoming of the model or its calibration, or caused by underestimating the return period and/or fracture depth of these specific events. Considering the weather conditions during the Vassdalen event (Lied, 1988) and the fall height of the Indre Standal avalanche, we conjecture that a high degree of fluidization increased the mobility of these avalanches. The Voellmy friction law adopted in RAMMS does not model this flow-regime transition, but an extended model with dynamically varying friction coefficients may significantly improve on this (Bartelt et al., 2012).

The commonly used friction parameter values lead to a drastic underestimation of the run-up height of the Gaukheidalen avalanche, but nearly perfect agreement with observations is obtained by using a high value of μ and nearly suppressing the drag term—a choice suggested by Gubler (1987) and later by Gauer et al. (2010) on the basis of detailed analyses of measured avalanche velocities. In the case of Indre Standal, however, this seems to lead to excessive velocities. This is not entirely surprising because RAMMS was mostly calibrated on data from quite large avalanches. Further case studies on natural deflecting dams will certainly help to improve the default parameterization.

Our study clearly shows that even advanced numerical models must be used with great care when *predicting* avalanche behavior at small scales and in complex terrain. However, when used with a criti-

cal mind they can give realistic answers to difficult problems like run-up heights. While model developers face the task of improving the velocity predictions of two-parameter models, avalanche consultants could contribute by sharing case studies similar to this with the user community. Finally, there is a long-standing need for a practical and verified methodology for estimating initial conditions of rare avalanches in different climates and topographic settings.

ACKNOWLEDGEMENTS. Data collection was financed by the European Commission (project CADZIE, contract nr. EVG1-CT-1999-0009). Data analysis and simulation were supported by the Norwegian Research Council through NGI project 581210 and by the Norwegian Water Resources and Energy Directorate through NGI projects 20100095, 20110114 and 20120154.

REFERENCES

Bartelt, P., Y. Bühler, O. Buser, M. Christen, and L. Meier. 2012. Modeling mass-dependent flow regime transitions to predict the stopping and depositional behavior of snow avalanches. *J. Geophys. Res.*, **117**, F01015.

Bühler, Y., M. Christen, J. Kowalski, and P. Bartelt. 2011. Sensitivity of snow avalanche simulations to digital elevation model quality and resolution. *Annals Glaciol.*, **52**(58), 72–80.

Buser, O. and H. Frutiger. 1980. Observed maximum runout distance of snow avalanches and the determination of the friction coefficients μ and ξ. *J. Glaciol.*, **26**(94), 121–130.

Casassa, G., H. Narita, and N. Maeno. 1989. Measurements of friction coefficients of snow blocks. *Annals Glaciol.*, **13**, 40–44.

Christen, M., J. Kowalski, and P. Bartelt. 2010. RAMMS: Numerical simulation of dense snow avalanches in three-dimensional terrain. *Cold Regions Sci. Technol.*, **63**(1-2), 1–14.

Christen, M., Y. Bühler, L. Schumacher, Y. Deubelbeiss, M. Salz, and P. Bartelt. 2011. RAMMS – A modeling system for snow avalanches in research and practice. User Manual v1.4 – Avalanche. Davos, Switzerland, WSL Inst. for Snow and Avalanche Research SLF.

Førland, E. J. 1992. Manual for beregning av påregnelige ekstreme nedbørverdier. Technical report. Oslo, Norway, Norwegian Meteorological Institute.

Gauer, P., K. Kronholm, K. Lied, K. Kristensen, and S. Bakkehøi. 2010. Can we learn more from the data underlying the statistical α-β model with respect to the dynamical behavior of avalanches? *Cold Regions Sci. Technol.*, **62**(1), 42–54.

Gruber, U. 1998. *Der Einsatz numerischer Simulationsmethoden in der Lawinengefahrenkartierung. Möglichkeiten und Grenzen*. PhD thesis, University of Zürich, Dept. of Geography, Zürich, Switzerland.

Gubler, H. 1987. Measurements and modelling of snow avalanche speeds. *In* Salm, B. and H. Gubler, editors, *Avalanche Formation, Movement and Effects (Proc. Davos Symposium, Sept. 1986), IAHS Publ. no. 162*. Wallingford, Oxfordshire, UK, IAHS Press, pages 405–420.

Harbitz, C. B. and U. Domaas. 1997. Mapping of natural deflecting dams. NGI Report 581210-1. Oslo, Norway, Norwegian Geotechnical Institute.

Harbitz, C. B. and U. Domaas. 2011. Functionality of deflecting dams and application of a centre-of-mass model. NGI Report 581210-2. Oslo, Norway, Norwegian Geotechnical Institute.

Irgens, F., B. Schieldrop, C. B. Harbitz, U. Domaas, and R. Opsahl. 1998. Simulations of dense-snow avalanches on deflecting dams. *Annals Glaciol.*, **26**, 265–271.

Lied, K. 1988. The avalanche accident at Vassdalen, Norway, 5 March 1986. *Cold Regions Sci. Technol.*, **15**(2), 137–150.

Lied, K and S Bakkehøi. 1980. Empirical calculations of snow-avalanche run-out distance based on topographic parameters. *J. Glaciol.*, **26**(94), 165–177.

Martinelli, Jr., M., T. E. Lang, and A. I. Mears. 1980. Calculations of avalanche friction coefficients from field data. *J. Glaciol.*, **26**(94), 109–119.

Salm, B., A. Burkard, and H. U. Gubler. 1990. Berechnung von Fliesslawinen. Eine Anleitung für Praktiker mit Beispielen. Mitteil. EISLF no. 47. Davos, Switzerland, Eidg. Institut für Schnee- und Lawinenforschung.

Sovilla, B., P. Burlando, and P. Bartelt. 2006. Field experiments and numerical modeling of mass entrainment in snow avalanches. *J. Geophys. Res.*, **111**, F03007.

Voellmy, A. 1955. Über die Zerstörungskraft von Lawinen. *Schweiz. Bauztg.*, **73**(12, 15, 17, 19), 159–165, 212–217, 246–249, 280–285.